Quantum Electronics **49** (12) 1149–1153 (2019)

https://doi.org/10.1070/QEL17164

Design principles for modern fibre-optic communication lines

V.A. Konyshev, O.E. Nanii, A.G. Novikov, V.N. Treshchikov, R.R. Ubaydullaev

Abstract. **We discuss the design issues and characteristics of coherent fibre-optic communication networks taking into account the many physical effects that simultaneously influence signal propagation. Algorithms and easy-to-use 'engineering' techniques are proposed that allow network performance to be predicted and the design to be significantly simplified.**

Keywords: *DWDM FOCL, required OSNR, BER, ASE noise, nonlinear noise, Gaussian noise, LOGO principle, coherent transmission system, line with chromatic dispersion compensators.*

1. Introduction

The ongoing development of the information society, the digitalization of all spheres of life and the deployment of new mobile communication technology (5G) lead a rapidly growing need for an increase in the amount and the rate of information transfer at all levels of optical networks [1, 2]. To increase the throughput of optical information transmission channels, conventional long-haul communication systems with data rates of 10 Gbit s^{-1} using amplitude modulation are replaced with coherent communication systems with data rates of 100 Gbit s^{-1} [3, 4].

Presently, 100G systems become dominant in long-haul communication networks and there is a transition to data rates of 200 and 400 Gbit s^{-1}. At the same time, the spectral efficiency and full capacity of DWDM communication networks increase.

The main difficulty that developers have to overcome while increasing the bandwidth of optical communication networks is the optical signal quality degradation due to the accumulation of amplifier noise, as well as linear and nonlinear signal distortions [5–7]. Forward error correction (FEC) and digital processing of received signals have begun to play a key role in modern high-speed communication systems, ensuring an increase in the quality of the services provided and reducing the cost of equipment and its operation [8, 9].

The propagation of informative optical signals is influenced by many physical phenomena in different spans of communication lines: attenuation and amplification, amplified spontaneous emission noise, chromatic dispersion, nonlinear distortion, stimulated Raman scattering, polarisation effects, spectral filtering and more. Thus, efficient design of cost-effective high-speed optical transmission systems and optical networks with constantly increasing throughput and geographical coverage is a major challenge. In this case, it is necessary to take into account the possibility of using a variety of modulation formats and coding algorithms (the combination of multi-level modulation and FEC is commonly called coded modulation).

Currently, the main physical phenomena that affect the propagation of signals in fibre-optic communication lines (FOCLs) have been revealed, and equations describing them have been proposed. However, in most practically important cases, the equations that determine the propagation of optical signals in FOCLs do not have analytical solutions, and correct numerical simulation requires large computational resources [10] and cannot always be used to design real networks and communication lines.

In addition, optical systems are gradually becoming more heterogeneous. Multi-span lines contain, as a rule, spans of different lengths, and different types of fibres can be used in different sections of the same line. In the designed networks, it is necessary to provide the ability to support transmission systems of different generations using different types of modulation formats and various symbol transmission rates.

Thus, the effective design and optimisation of a complex optical communication network is a very sophisticated, multifaceted and voluminous problem. Its solution includes the selection of the necessary active and passive optical, electronic and optoelectronic components, the optimal integration of all components, nodes and subsystems into a single network and, finally, the finding of the optimal operating parameters of all components. The calculation of each configuration by solving the equations of propagation of light signals in FOCLs requires time-consuming calculations on supercomputers, which makes multiparameter optimisation almost impossible.

It is impossible to cope with the complexity of design without the use of relatively simple (suitable for analysis) models and algorithms, which make it possible to obtain a fair, general, approximate, but fairly accurate, estimate of network performance, reliability and operating margin, as well as the costs of putting it into operation.

In this paper, we analyse the well-known approaches to the prediction of characteristics, discuss the areas of their

V.A. Konyshev, A.G. Novikov, R.R. Ubaydullaev T8 LLC, Krasnobogatyrskaya ul. 44/1, office 826, 107076 Moscow, Russia; e-mail: rru@t8.ru;
O.E. Nanii T8 LLC, Krasnobogatyrskaya ul. 44/1, office 826, 107076 Moscow, Russia; Faculty of Physics, Lomonosov Moscow State University, Vorob'evy Gory, 119991 Moscow, Russia;
V.N. Treshchikov T8 LLC, Krasnobogatyrskaya ul. 44/1, office 826, 107076 Moscow, Russia; Kotel'nikov Institute of Radioengineering and Electronics (Frayzino Branch), Russian Academy of Sciences, pl. Akad. Vvedenskogo 1, 141190 Fryazino, Moscow region, Russia

Received 18 October 2019
Kvantovaya Elektronika **49** (12) 1149–1153 (2019)
Translated by I.A. Ulitkin

applicability, within which the required accuracy is ensured, and propose a consistent algorithm for designing fibre-optic long-haul communication networks. The need for constant verification of the accuracy and applicability of the models by comparing them with the results of physical and/or numerical experiments is shown.

2. Signal degradation due to amplified spontaneous emission noise and nonlinear effects

In linear propagation mode, the quality of the optical signal is degraded due to the accumulation of amplified spontaneous emission (ASE) noise in erbium-doped fibre amplifiers (EDFAs). The transmission range is limited by the fact that as the ASE noise power increases, the optical signal-to-noise ratio $OSNR_{\mathrm{L}}$ in the line decreases and at a maximum range it is compared with the maximum allowable $OSNR_{\mathrm{R}}$ value. In the absence of nonlinear distortions, $OSNR_{\mathrm{R}}$ is the same as $OSNR_{\mathrm{BTB}}$ (the $OSNR_{\mathrm{R}}$ value in the back-to-back configuration). Linear distortions (chromatic dispersion and polarisation mode dispersion) practically do not affect the performance of coherent communication systems, since such distortions are compensated for by digital signal processing in a coherent receiver.

The value of $OSNR_{\mathrm{R}}$ in the real line is noticeably greater than that of $OSNR_{\mathrm{BTB}}$. The difference between $OSNR_{\mathrm{R}}$ in a real line and $OSNR_{\mathrm{BTB}}$ (both values are expressed in decibels) is called the 'OSNR penalty' for that line. The reason for the occurrence of this penalty is the degradation of the optical signal under the influence of nonlinear effects.

The nature of the action of nonlinear effects in FOCLs is significantly different in lines containing dispersion compensators at the physical level (DC lines), and in modern coherent lines without compensators (NDC lines). In short and long FOCLs with dispersion compensators, nonlinear effects are manifested mainly in the form of distortions in the shape of the transmitted optical signals. In lines without optical compensation of chromatic dispersion, the mechanism of nonlinear signal degradation turns out to be significantly different and can be described as the occurrence and accumulation of nonlinear interference noise. The design of FOCLs with dispersion compensators using receivers with direct detection and channel rates of 10 and 40 Gbit s^{-1} is extensively described in the literature reviewed in [1, 11]. However, the methods presented in this literature are not applicable to coherent communication systems with rates of 100 Gbit s^{-1} or higher, using optical lines without dispersion compensation.

In fibre-optic information transmission systems without periodic dispersion compensation, the optical field becomes random due to dispersion effects, leading to a spatial overlap of many transmitted symbols. Due to the large accumulated dispersion, the influence of nonlinear effects is weakened, becomes random, and manifests itself as nonlinear noise during detection [12–16].

The method for calculating ASE noise in optical communication lines with EDFAs is well known [1]. The signal powers and ASE noise at the EDFA output are related to the signal powers and ASE noise at its input by the expressions:

$$P_{\mathrm{out}} = P_{\mathrm{in}} G, \tag{1}$$

$$P_{\mathrm{ASE\,out}} = P_{\mathrm{ASE\,in}} G + (FG - 1) h\nu B, \tag{2}$$

where P_{in} and P_{out} are the signal powers at the input and output of the EDFA; $P_{\mathrm{ASE\,in}}$ and $P_{\mathrm{ASE\,out}}$ are the noise powers at the input and output of the EDFA in a reduced bandwidth B, which is considered to be equal to 12.5 GHz; G and F are the EDFA gain and noise factor; ν is the carrier frequency; and h is Planck's constant. The optical signal-to-noise ratios at the input ($OSNR_{\mathrm{L\,in}}$) and output ($OSNR_{\mathrm{L\,out}}$) of the EDFA in the bandwidth B are related by the expression

$$\frac{1}{OSNR_{\mathrm{L\,out}}} = \frac{1}{OSNR_{\mathrm{L\,in}}} + \frac{1}{OSNR_{\mathrm{EDFA}}}, \tag{3}$$

where

$$OSNR_{\mathrm{EDFA}} = \frac{P_{\mathrm{in}}}{h\nu B(F - 1/G)} \approx \frac{P_{\mathrm{in}}}{h\nu BF}. \tag{4}$$

With large accumulated dispersion, the nonlinear interaction in a FOCL span generates nonlinear noise with a power P_{NL} [9–13], which is additively added to the ASE noise. The power of accumulated nonlinear noise, recalculated at the entrance to the span, is proportional to the cube of the signal power at the entrance to the span:

$$P_{\mathrm{NL}} = \eta P^3, \tag{5}$$

where η is the nonlinearity coefficient, depending on the fibre and signal parameters.

Similarly to the above-introduced $OSNR_{\mathrm{L}}$ value, related to the ASE noise power, we introduce the $OSNR_{\mathrm{NL}}$ value related to the nonlinear noise power:

$$OSNR_{\mathrm{NL}} = \frac{P}{P_{\mathrm{NL}}}. \tag{6}$$

3. Required OSNR value and OSNR margin

For the quantitative determination of the stability of a communication system to the degradation of FOCL characteristics, most telecom operators use the concept of OSNR margin, the value of which, $OSNR_{\mathrm{M}}$, is determined by the expression

$$OSNR_{\mathrm{M}} = \frac{OSNR_{\mathrm{L}}}{OSNR_{\mathrm{R}}}, \tag{7}$$

where the $OSNR_{\mathrm{R}}$ value is called the required OSNR and is measured as follows. First, the OSNR at the end of the DWDM line ($OSNR_{\mathrm{L}}$ value) is measured with a spectrum analyser (Fig. 1). Then, ASE noise is added to the line until the line stops working. The OSNR in the line, measured using a spectrum analyser, is called the required OSNR ($OSNR_{\mathrm{R}}$).

The OSNR margin measurement scheme includes: two BER testers (BERT1 and BERT2), the first of which forms a reference test sequence, and the second receives it and determines the signal error rate; transponders (TP1 and TP2); a multiplexer and a demultiplexer (MUX and DEMUX); a DWDM line consisting of erbium-doped fibre amplifiers (EDFAs) and sections of optical fibre; a source of amplified spontaneous emission (ASE); an optical spectrum analyser (OSA); a variable optical attenuator (VOA); and splitters (90×10 and 99×1).

The line is operational when the condition

$$OSNR_{\mathrm{M}} > 1 \tag{8}$$

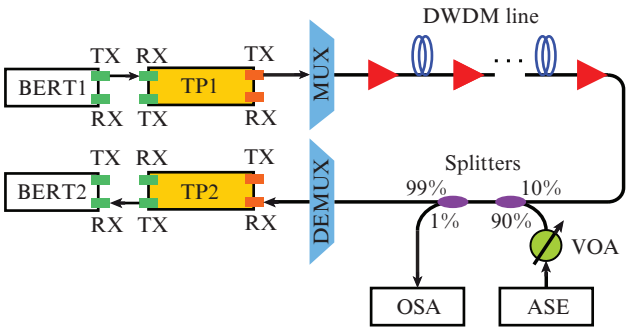

Figure 1. Scheme for measuring the OSNR margin in the line.

is met. However, when putting the line into operation, it is necessary to fulfil a more stringent condition:

$$OSNR_{\mathrm{M}} > 2. \tag{9}$$

4. Models of noise accumulation in a line with optical amplifiers

If we assume that the nonlinear distortions are described by nonlinear noise, which is additively added to linear noise, then the total noise power in the line will be determined by the expression

$$P_{\Sigma} = P_{\mathrm{ASE}} + P_{\mathrm{NL}}. \tag{10}$$

Dividing both sides of (10) by the signal power at a given point P, we obtain

$$\frac{1}{OSNR_{\mathrm{BER}}} = \frac{1}{OSNR_{\mathrm{L}}} + \frac{1}{OSNR_{\mathrm{NL}}}, \tag{11}$$

where $OSNR_{\mathrm{BER}} = P/P_{\Sigma}$ is the ratio that determines the bit error rate (BER), which is measured by the transponder before it performs forward error correction. The relationship between $OSNR_{\mathrm{BER}}$ and BER in this model is one-to-one and is described by the transponder calibration curve. The calibration curve refers to the dependence of $\lg BER$ on $OSNR_{\mathrm{BER}}$, obtained experimentally in the linear mode of line operation (in this case, $P_{\mathrm{NL}} = 0$, and therefore $OSNR_{\mathrm{BER}} = OSNR_{\mathrm{L}}$). This dependence is used to determine $OSNR_{\mathrm{BER}}$ by the BER level in the nonlinear mode. The method for constructing the calibration curve is given in Section 4.

To describe a multi-span DWDM line, we introduce some notations (Fig. 2). Conventionally, the line can be divided into sections (total N spans), each of which consists of a fibre span and an EDFA. Section n (n = 1, ..., N) is characterised by the following parameters: P_n, A_n, η_n, G_n, and F_n, which are, respectively, the launched signal power, transmission losses of the fibre, nonlinearity coefficient, gain and noise figure of the amplifier for the nth sections of the DWDM line.

Due to the additive addition of ASE noise from different EDFAs, the expression for the total inverse OSNR in the line due to ASE noise has the form [the first term in relation (11)] (Fig. 2)

$$\frac{1}{OSNR_{\mathrm{L}}} = \sum_{n=1}^{N} \frac{1}{OSNR_{\mathrm{L}n}} = \sum_{n=1}^{N} \frac{h\nu BA_nF_n}{P_n}. \tag{12}$$

Assuming that the nonlinear noise from different spans is added additively, taking into account (5), we obtain the simple analytical expression for the inverse nonlinear OSNR in a multi-span line (Fig. 2), convenient for calculating the communication line [1, 12–14]:

$$\frac{1}{OSNR_{\mathrm{NL}}} = \sum_{n=1}^{N} \frac{1}{OSNR_{\mathrm{NL}n}} = \sum_{n=1}^{N} \eta_n P_n^2. \tag{13}$$

Thus, $OSNR_{\mathrm{BER}}$ is defined by the expression

$$\frac{1}{OSNR_{\mathrm{BER}}} = \sum_{n=1}^{N} \left(\frac{h\nu BA_nF_n}{P_n} + \eta_n P_n^2 \right). \tag{14}$$

Formula (14) is very convenient for the design and optimisation of communication lines. The problem is reduced to finding the minimum of the $OSNR_{\mathrm{BER}}^{-1}$ function with varying powers P_n for fixed values of A_n, η_n, G_n and F_n. From formula (14), which is the sum of independent pairs of terms in separate spans of the line, there follows the LOGO principle, i.e. local optimisation leads to global optimisation. From (14), it is easy to obtain an explicit analytical expression for the optimal power in each span at which the minimum $OSNR_{\mathrm{BER}}^{-1}$ is achieved:

$$P_n = \left(\frac{h\nu BA_nF_n}{2\eta_n} \right)^{1/3}. \tag{15}$$

Adding a span or changing span parameters does not affect the optimal power of the remaining spans.

The nonlinear additive (incoherent Gaussian) noise model (IGN model) is very convenient for the design of communication lines, and it is advisable to use it whenever it provides a given accuracy. For practical application of the model, it is necessary to measure or calculate the nonlinearity coefficients η_n for spans. Due to the correlation between nonlinear distortions generated in different spans, the additive model does not give a very accurate result.

In a real line, noise grows faster with an increase in the number of DWDM sections. A positive correlation in the accumulation of nonlinear noise is taken into account by the ε-model, in which the total nonlinear OSNR in the line is determined by the relation

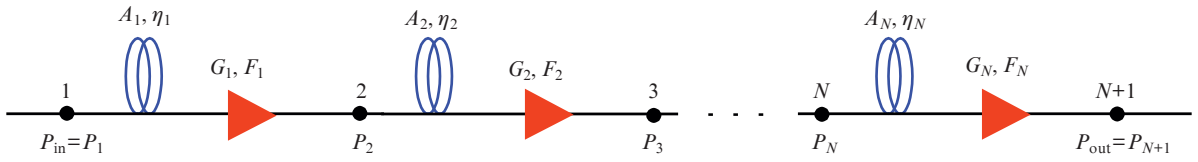

Figure 2. Parameters of components and optical signal of a multi-span line with EDFAs.

$$\frac{1}{OSNR_{\mathrm{NL}}} = \left[\sum_{n=1}^{N}\left(\frac{1}{OSNR_{\mathrm{NL}\,n}}\right)^{1/(1+\varepsilon)}\right]^{1+\varepsilon}, \qquad (16)$$

where the dimensionless parameter ε is calculated experimentally.

5. Experimental determination of model parameters

The experimental part of the work consists in performing a series of measurements that make it possible to determine the nonlinearity coefficients η of optical spans and other constants included in the analytical formulas for calculating the parameters of the communication line. The experimental setup is shown in Fig. 3. It includes: a BER tester (BERT); a coherent transponder (TP); a multiplexer and a demultiplexer (MUX and DEMUX); input and output erbium-doped fibre amplifiers ($\mathrm{EDFA_{in}}$ and $\mathrm{EDFA_{out}}$) operating in a constant power out mode; a multi-section model of a DWDM line, consisting of coils of an optical single-mode fibre (A_n loss) and erbium-doped fibre amplifiers (EDFA_n) operating in a constant gain mode; a source of amplified spontaneous emission (ASE); an optical spectrum analyser (OSA); variable optical attenuators ($\mathrm{VOA_{in}}$ and $\mathrm{VOA_{ASE}}$); and splitters (90×10 and 99×1).

When constructing the calibration curves, the communication line shown in square brackets in Fig. 3 was replaced by a short length of fibre (a patch cord less than 3 m long). Using $\mathrm{VOA_{ASE}}$, the power of the additional ASE noise changes; in this case, the transponder measures *BER*, and the spectrum analyser measures $OSNR_{\mathrm{L}}$. The $OSNR_{\mathrm{L}}$ value in the back-to-back configuration is the same as the $OSNR_{\mathrm{BER}}$ value. An example of calibration curves for two transponders – Volga and Kuban (T8 LCC), which differ in the shape of the radiation spectrum, is shown in Fig. 4.

In determining the nonlinearity coefficient of the *N*-span line, the ASE noise source was turned off. The dependence of BER at the transponder on the input power P_{in} at point 1 was measured (Fig. 3). The power at this point was changed using the digital variable optical attenuator $\mathrm{VOA_{in}}$, which shows the amount of introduced losses (previously, the power was measured at point 1 by connecting the OSA at this point). The $\mathrm{EDFA_{out}}$ amplifiers operated in a constant gain mode, the gain being chosen so as to compensate for the loss in spans (spans of 100 km in length). This ensures that P_{in} powers introduced across all spans are equal. The $\mathrm{EDFA_{out}}$ amplifier, in contrast, operated in a constant power out mode to provide optimal power at the transponder input. Also, at each step, the OSNR value in the line was measured using OSA. Thus, the dependences of $OSNR_{\mathrm{NL}}^{-1}$ [$OSNR_{\mathrm{NL}}^{-1} = OSNR_{\mathrm{BER}}^{-1}(BER) - OSNR_{\mathrm{L}}^{-1}$] on P_{in} were constructed.

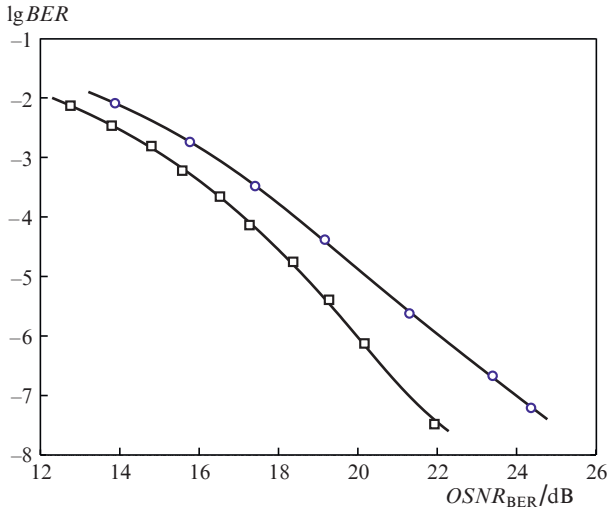

Figure 4. Calibration curves for (○) Volga and (□) Kuban transponders (100 Gbit s^{-1}, DP-QPSK modulation format). The solid curves are the cubic approximation of the experimental data.

An example of the experimental determination of the nonlinearity coefficients η (the slope of the dependence of $OSNR_{\mathrm{NL}}^{-1}$ on P_{in}^2)) for a single-span line is shown in Fig. 5.

To verify the mathematical apparatus, the characteristics of many configurations are experimentally measured, which are compared with the characteristics obtained by calculation using the mathematical apparatus.

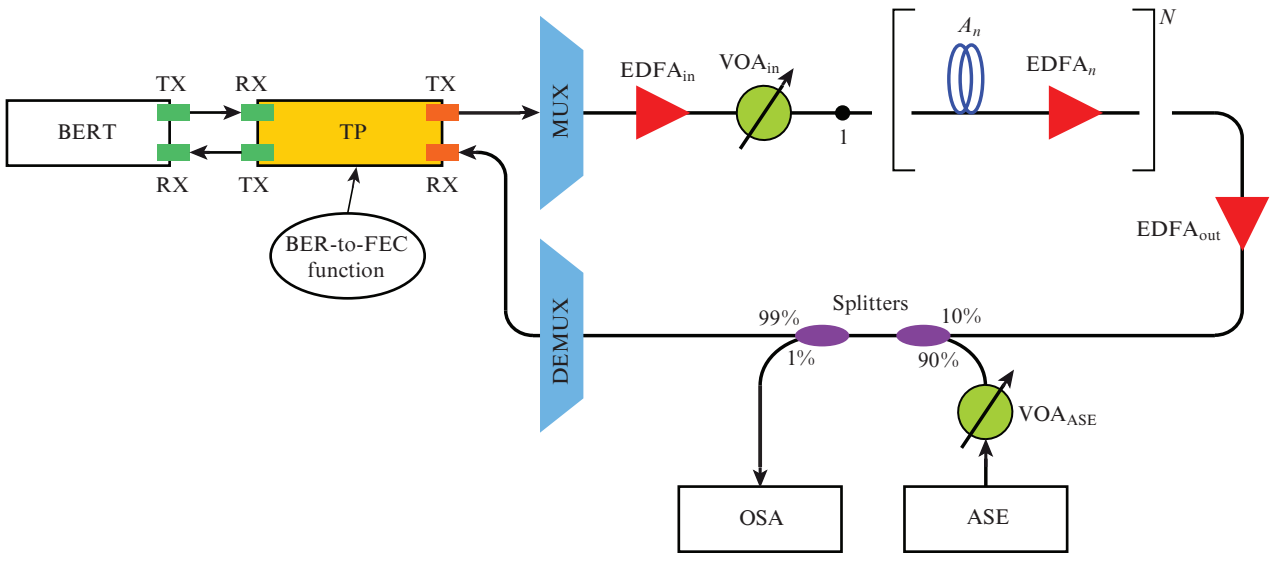

Figure 3. Experimental setup for determining the calibration curve of transponders and nonlinearity coefficients of the communication line.

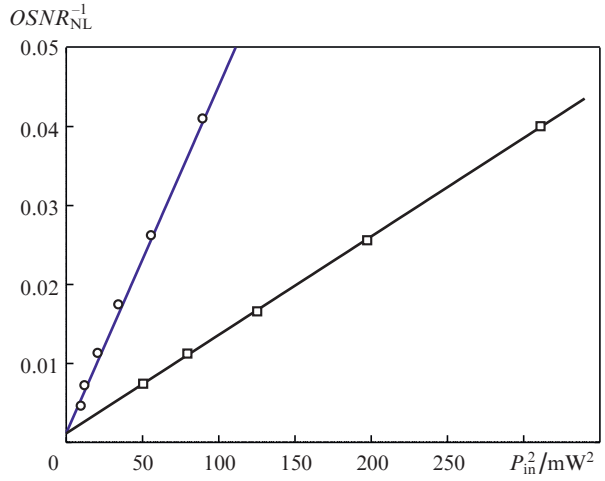

Figure 5. Dependences of $OSNR_{NL}^{-1}$ on P_{in} for the experimental determination of the coefficient η for (○) Volga and (□) Kuban transponders ($N = 1$, $L = 100$ km).

It was found that the deviations of the calculated values of the required OSNR from the experimental values for all the studied configurations are in a given range: a positive deviation of 0.12–0. 76 dB, while for lines with spans 100 km long, the ε value lies in the range 0.2–0.3.

Thus, the ε model provides high accuracy of calculations; however, the method for determining the parameter ε is a sophisticated experimental problem, which complicates the practical application of this model. Therefore, in all cases when the required accuracy allows this, it is necessary to use the additive model.

6. Conclusions

We have described simple design principles for complex heterogeneous FOCLs typical of terrestrial telecommunication systems (regional, interregional, national and international). The most effective strategy for planning fibre-optic lines and communication networks is a two-stage design process.

It is advisable to carry out preliminary design and initial comparative analysis of various options for the implementation of FOCLs using approximate calculation algorithms. For this stage, the approximation of additive incoherent Gaussian noise provides sufficient accuracy. The results obtained at this stage can be used to assess the total cost of a network that provides a given bandwidth and satisfies other requirements and limitations.

When preparing the final design documentation, it is advisable to analyse and optimise the technical and economic characteristics of the FOCL using a more accurate ε model.

References

1. Listvin V.N., Treshchikov V.N. *DWDM-sistemy (DWDM Systems)* (Moscow: Tekhnosphera, 2017).
2. Winzer P.J., Neilson D.T., Chraplyvy A.R. *Opt. Express*, **26** (18), 24190 (2018).
3. Nanii O.E., Treshchikov V.N. *T-Comm: Teleckommunikatsiya i Transport*, **8**, 76 (2011).
4. Saunders R. *Opt. Fiber Technol.*, **17** (5), 445 (2011).
5. Zhitelev A.E. et al. *Quantum Electron.*, **47**, 1135 (2017) [*Kvantovaya Elektron.*, **47**, 1135 (2017)].
6. Burdin V.A. et al. Quantum Electron., **47**, 1144 (2017) [*Kvantovaya Elektron.*, **47**, 1144 (2017)].
7. Sidelnikov O.S. et al. *Quantum Electron.*, **47**, 1147 (2017) [*Kvantovaya Elektron.*, **47**, 1147 (2017)].
8. Alvarado A. et al. *J. Lightwave Technol.*, **36** (2), 424 (2018).
9. Ishida O., Takei K., Yamazaki E. *Proc. 2016 Optical Fiber Communications Conf. and Exhibition* (OFC) (Anaheim, 2016).
10. Yushko O.V. et al. *Quantum Electron.*, **45** (1), 75 (2015) [*Kvantovaya Elektron.*, **45** (1), 75 (2015)].
11. Antona J.C., Bigo S. *Comptes Rendus Physique*, **9** (9-10), 963 (2008).
12. Poggiolini P. *J. Lightwave Technol.*, **30** (24), 3857 (2012).
13. Torrengo E. et al. *Proc. ECOC* (Geneva, 2011) We.7.B.2.
14. Vacondio F. et al. *Proc. ECOC* (Geneva, 2011) We.7.B.1.
15. Gurkin N.V. et al. *Quantum Electron.*, **43** (6), 550 (2013) [*Kvantovaya Elektron.*, **43** (6), 550 (2013)].
16. Gainov V.V. et al. *Laser Phys. Lett.*, **10**, 075107 (2013).